Out-of-Band Exposure Characterization with the SEMATECH Berkeley 0.3-NA Microfield Exposure Tool

Simi A. George, Patrick P. Naulleau, Senajith Rekawa, Eric Gullikson
and Charles Drew Kemp

Center for X-ray Optics, Lawrence Berkeley National Laboratory
1 Cyclotron Road, Berkeley, CA 94720

ABSTRACT

For the commercialization of extreme ultraviolet lithography (EUVL), discharge or laser produced, pulsed plasma light sources are being considered. These sources are known to emit into a broad range of wavelengths that are collectively referred to as the out-of-band (OOB) radiation by lithographers. Multilayer EUV optics reflect OOB radiation emitted by the EUV sources onto the wafer plane resulting in unwanted background exposure of the resist (flare) and reduced image contrast. The reflectivity of multilayer optics at the target wavelength of 13.5 nm is comparable to that of their reflectivity in the deep ultraviolet (DUV) and UV regions from 100-350 nm. The aromatic molecular backbones of many of the resists used for EUV are equally absorptive at specific DUV wavelengths as well. In order to study the effect of these wavelengths on imaging performance in a real system, we are in the process of integrating a DUV source into the SEMATECH Berkeley 0.3-NA Microfield Exposure Tool (MET). The MET plays an active role in advanced research in resist and mask development for EUVL and as such, we will utilize this system to systematically evaluate the imaging impact of DUV wavelengths in a EUV system. In this paper, we present the optical design for the new DUV component and the simulation-based imaging results predicting the potential impact of OOB based on known resist, mask, and multilayer conditions. It should be noted that because the projection optics work equally well as imaging optics at DUV wavelengths, the OOB radiation cannot be treated simply as uniform background or DC flare.

Keywords: Out-of-band, EUVL, MET, Extreme Ultraviolet, Out of band, Resists, Flare, resist sensitivity

1. INTRODUCTION

Extreme Ultraviolet Lithography[1] (EUVL) is the candidate technology currently under development for computer chip production at the 22 nm node and below.[2] The wavelength chosen for the tool architectures is 13.5 nm. Since radiation at these wavelengths are strongly absorbed by all materials, EUVL systems will utilize all reflective optics, specifically, Mo-Si dielectric mirrors. The light sources generating this wavelength for EUVL will be either discharge or laser plasmas. The large density gradients existing in plasmas lead to photon emissions into a broad range of wavelengths; from EUV to IR. In the case of laser plasmas, scattering of the heating laser by the dense plasmas is also expected. Out-of-band (OOB) is a general term used by the EUVL community to describe any radiation that is emitted outside required bandwidth (BW) of the wavelength needed for patterning. This lack of the spectral purity of the light source is a concern for lithographers. The Mo-Si multilayer mirrors (MLMs) selects a narrow, 2% FWHM BW centered at 13.5 nm from the source in the EUV region, while absorbing or reflecting the broader source spectral emission. This leads to problems such as mirror heating resulting in interdiffusion of multilayers, photon assisted oxidation and contamination and flare at the wafer.[3] While the first two mechanisms result in mirror reflectivity loss and reduced component lifetime, the latter affects the critical dimension (CD) control in patterning by exposing the photoresists.[3]

EUV resists are based on resist molecular platforms designed for lithographic exposures at either 193 nm or 248 nm and they are sensitive to the wavelengths between 100-400 nm (DUV/UV). Reduced aerial image contrast as a result of resist exposure to source radiation into the DUV/UV reaching the wafer is expected. The

Send correspondence to Simi George and Patrick Naulleau
Simi George: E-mail: sageorge@lbl.gov, Telephone: 1 510 486 6902
Patrick Naulleau: E-mail: pnaulleau@lbl.gov, Telephone: 1 510 486 4529

maximum allowed budget for DUV/UV tolerable at wafer for a production ready stepper system, as listed by the tool manufacturers,[4] is limited to less than 1%. For this paper, we will concentrate on evaluating flare effects due to these wavelengths exposing the photoresists. We will present in detail, the methodology used for evaluating DUV/UV throughput to wafer and the effective flare causing aerial image contrast reduction.

2. CALCULATING DUV/UV THROUGHPUT TO WAFER

A simple model can be used to determine how much DUV/UV radiation reaches the wafer in a typical EUVL production type stepper design. The basis for the assumptions used in the calculations are also presented. Two cases of proposed EUVL stepper optical layouts are considered in the calculation of the optical transmission to wafer and to make flare comparisons. The first case considered uses eleven total reflections from illuminator entrance to the wafer, where two of the eleven reflections are at grazing incidence.[5] For the purposes of calculation here, we assume that the glancing mirrors are Ruthenium coated and at 15 degrees angle of incidence. Another proposed layout uses 10 total reflections with one grazing mirror at 10 degrees angle of incidence.[6] We will assume that the grazing mirror coating is Ruthenium for the 10 mirror design as well. For these calculations, we are also assuming perfect bandwidth match between all mirrors, which might not be case in the real systems. Tool specifications tolerance bandwidth mismatch at a maximum of 5%.[3] Flare resulting from imaging by OOB is determined by using the resist sensitivity to the different wavelengths transmitted to wafer.

2.1 DUV/UV Emission Contribution from Plasma Sources

The amount of DUV/UV emission expected at the intermediate focus (IF), the pseudo illumination focal point in the EUVL stepper system, is still open to debate. In 2004, SEMATECH lead studies found a Xe discharge plasma source emission into a bandwidth from 160 nm to 325 nm to be approximately 12% of IF EUV power and that a droplet based Sn laser plasma emits approximately 10% into 160-715 nm bandwidth.[7,8] A recent study from the institute of laser engineering (ILE) at Osaka in Japan is reporting more than 22% emission into 100-400 nm, for a 100 nm Sn sphere target (Fig. 1).[9,10] Any photon emission from a given plasma source is highly dependent on the source element(s), size, and geometry, as well as the plasma temperature and density. In certain configurations there is an angular distribution to the light generated, thus the amount of radiation at IF depends on the geometry of light collection. For this study, we assume that it may be possible to have anywhere from 10%-20% DUV/UV at IF for a production ready source without any spectral purity filters. Emission profile will depend on source conditions. In the calculations completed here, the published Sn spectral profile from ILE Osaka[9,10] is used for both 10% and 20% DUV/UV assumption.

2.2 Mirror Reflectivity

For determining power throughput to wafer broadband reflectance of the mirrors in the optical system is needed. The optical constants used for modeling the reflectance for the mirrors is obtained from Palik's Handbook of Optical Constants.[11,12] Modeled reflectance data for the two types of mirrors used for the stepper optical layouts are given in figures 2 and 3. Figure 4 shows measured reflectance for a Ru capped Mo-Si mirror provided by outside source. Peak EUV reflectivity for the modeled and the measured mirror data is near 65%, while the broad band data exhibit differences. EUV reflectance for the grazing mirror is greater than 80%. The measured and modeled data show that the optics are equal or better reflectors for a large range of wavelengths.

2.3 Transmitted Power to Wafer

The simple method for calculating optical transmission to wafer from IF of the stepper, without taking into consideration any reflectivity changes due to changes in the incidence angles and bandwidth mismatch, can be given by accounting for the total number of reflections as

$$OTF(\lambda) = [R_M(\lambda)]^{\#\ of\ reflect.} \times [R_G(\lambda)]^{\#\ of\ reflect.} \quad (1)$$

where R_M is the reflectivity of the multilayer mirrors and R_G is the reflectivity of the grazing incidence mirrors. The optical transfer to wafer calculated for the two different optical layouts considered for the modeled and measured mirror data are shown in figures 5 and 6, respectively. In figure 5, the OOB reflectivity peaks between

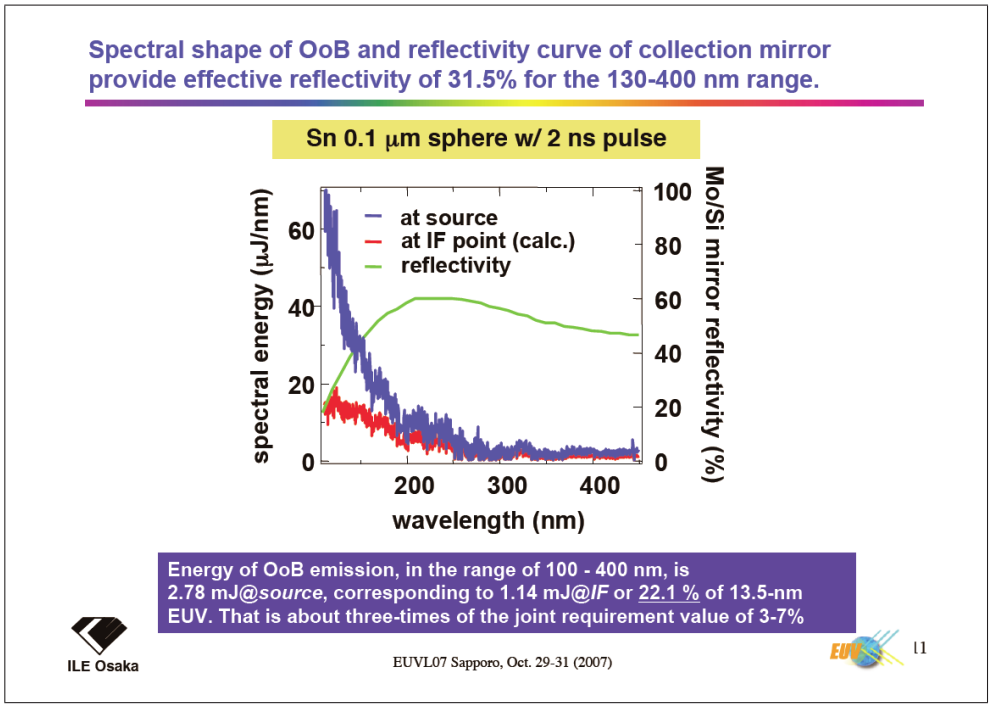

Figure 1: Recent study for Sn OOB data presented at EUVL in Sapporo, 2007

250 nm and 300 nm and the integrated area is very large in comparison to EUV. This data here is modeled for an ideal Mo-Si dielectric structure with Si as the final layer and without taking into account layer roughnesses, interdiffusion or other possible factors that may affect OOB reflectivity. Typically, dielectric mirrors employed in optical systems employ a capping layer in order to control oxidation and there might be a sacrificial separation layer between substrate and multilayers[13] where these layers alter the reflectivity characteristics of the mirror in the DUV/UV. Transmission to wafer for a Ru-capped (thickness unknown) Mo-Si mirror used in an EUVL system is given in figure 6. The DUV wavelengths shows greater suppression and UV band height is reduced when compared to EUV peak height.

Once we have optical transmission to the wafer using the reflectivity data, the power at the wafer can be determined for the EUV bandwidth. Assuming 180W of EUV is collected at IF, we can apply spectral information to the mirror reflectivity and integrate as follows,

$$P(EUV_{2\%BW})\,(W) = 180W \int_{\lambda_1}^{\lambda_2} OTF(\lambda)S(\lambda)d\lambda \tag{2}$$

where $S(\lambda)$ is the source emission spectrum obtained from the source. For these calculations, published spectral data for a Sn sphere based EUV light source was used. The power transfer to wafer in the 100 nm-400nm region is calculated in the same way, except now we are assuming that either 10% or 20% of the EUV input at IF is collected. For 180W of EUV, at 10% we can expect,

$$0.1 \times P(EUV_{2\%BW})\,(W) = 18W = P(OOB) \int_{\lambda_{100}}^{\lambda_{400}} S(\lambda)d\lambda \tag{3}$$

for the OOB spectral distribution of a given source. For the calculations here, published data based on a 10 μm Sn sphere source for wavelengths up to 400 nm was used[9] which is shown in figure 7. Previous calculations assume uniform UV illumination across the DUV/UV region or a blackbody emission profile for a given plasma temperature[14] which is not the case for a real source with temperature gradients. Collected radiation, again, depends on the source generation conditions and the amount of reflected radiation varies according to the

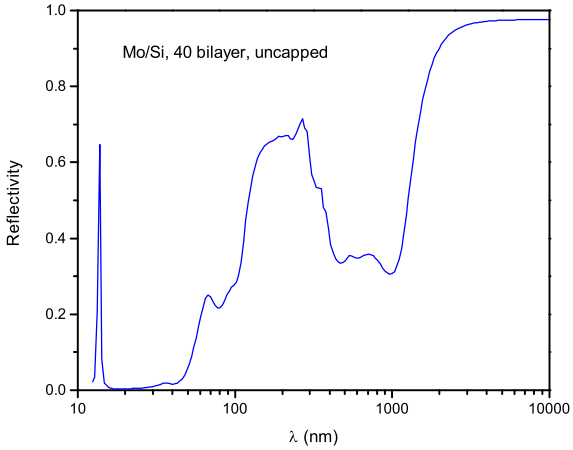

Figure 2: Calculated mirror reflectivity for a 40 layer, Mo-Si mirror out to 10 μm.

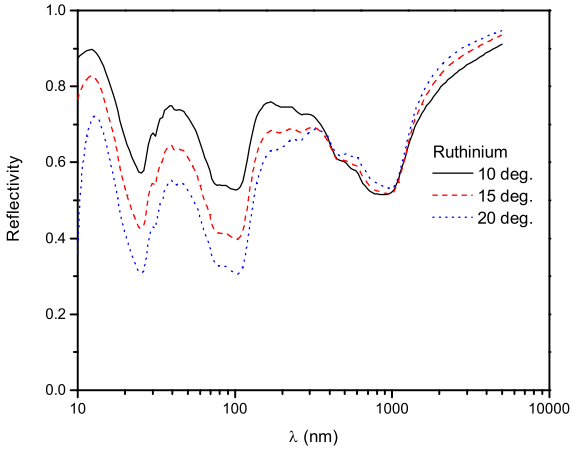

Figure 3: Calculated reflectivity data for Ru coatings at three different angles of incidence.

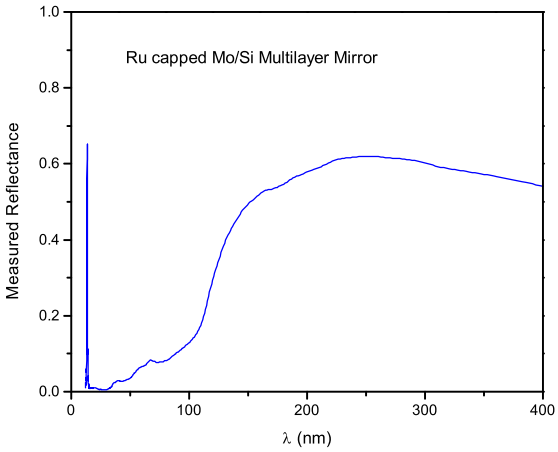

Figure 4: Measured reflectance data for a Ru capped, Mo-Si MLM to 400 nm.

emission profile. If we were to better account for the resist sensitivity to wavelengths and estimate flare, then source emission profile is a key factor and should be known. To isolate power into smaller bandwidths of interest in the DUV/UV wavelength region,

$$P(OOB_{wafer})\,(W) = 18W \int_{\lambda_1}^{\lambda_2} OTF(\lambda)S(\lambda)d\lambda \tag{4}$$

where λ_1 and λ_2 can be the bandwidth of interest. The source power transmission to wafer calculated with modeled and measured mirror data is shown in figure 8 for all cases considered in this study. The modeled mirror reflectivity transfer to the wafer is orders of magnitude greater than the measured mirror into the OOB. For all further calculations, we will utilize the measured Ru-capped, Mo-Si mirror data.

The integrated power into the entire 100-400 nm region is compared to the full integrated EUV band at wafer. For the 11 mirror system, DUV/UV is estimated to be 3.1% of the EUV and for the 10 mirror system, it is 4.2% assuming that at IF 10% of the EUV was collected into these wavelengths. For 20% OOB, these values simply

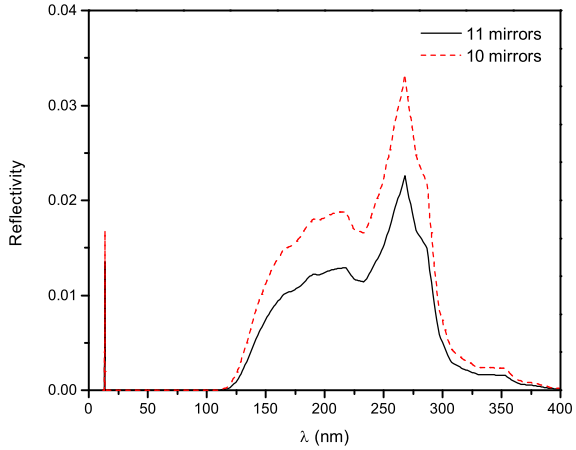

Figure 5: Optical transmission to wafer for the modeled, uncapped Mo-Si mirrors. The reflectivity peaks in the UV region between wavelengths 250 nm and 300 nm.

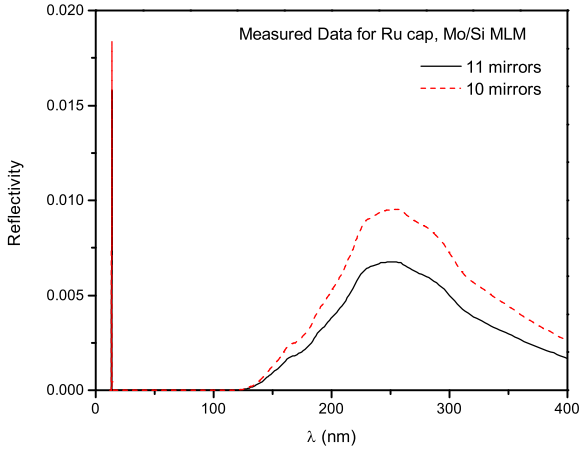

Figure 6: Transmission to wafer on the measured data for the Ru-capped Mo-Si mirrors. Longer wavelengths are better suppressed here as compared to the nodeled data.

double. The estimate will vary depending on the capping layer materials and thicknesses used, other coatings the mirrors may have and with any bandwidth mismatch.

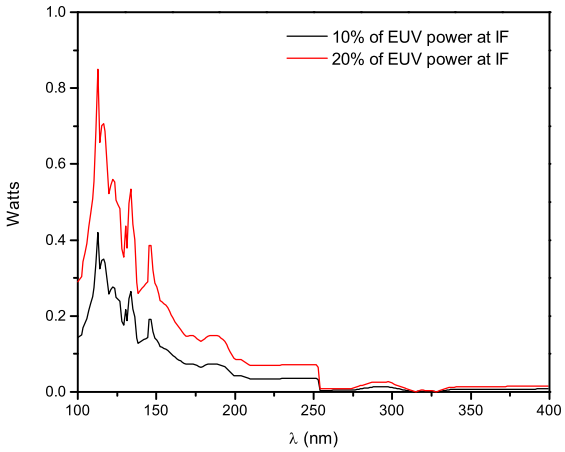

Figure 7: Source spectral distribution extracted from published data[9] for OOB at 10% and 20% of EUV.

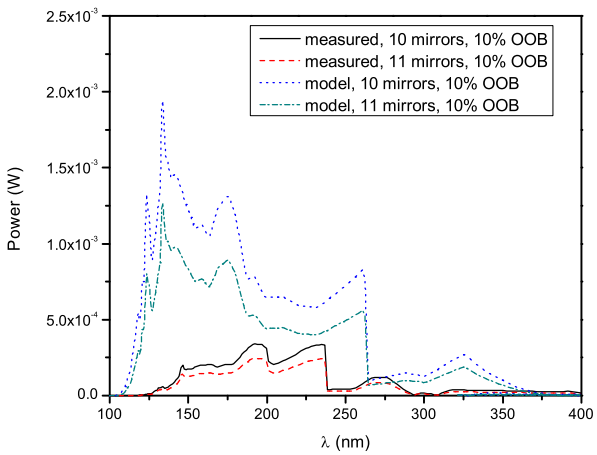

Figure 8: Source power at the wafer for modeled and measured mirror for OOB at 10% and 20% of EUV.

2.4 Calculated Resist Dependent Flare

EUV photoresists for mask pattern transfer have evolved from previous and existing resist platforms at 248 nm and 193 nm. Common ingredients in photoresist samples are typically polymer, photoacid generator(PAG), quencher, ethyl lactate and propylene glycol monomethyl ether acetate; all are molecular compounds absorbing in the DUV/UV region. To further sensitize the resists so that less photons are required to induce photochemical processes, chemical amplification is utilized. In chemically amplified resists, a catalytic species generated by irradiation lowers the kinetic energy threshold for subsequent chemical transformations, thus providing a gain

mechanism and the process works for both EUV and DUV wavelengths.[15] EUV resist response in the DUV/UV region depends on the absorption profiles of the resist platforms and varies across wavelengths and with thickness.[16] It is possible for a resist to have high absorption for wavelengths, while requiring high clearing dose for the same wavelengths if the resist is too thick. To maintain resist transparency at EUV, typical thicknesses used currently are 60 nm or 80 nm. There are some thickness variations with various features, which will affect OOB flare contribution as well. The effective OOB flare should depend on the resist sensitivity to these wavelengths relative to the EUV for a given resist at a given film thickness. This can be estimated as described.

The sensitivity to various wavelengths relative to EUV was determined by comparing supplier provided clearing dose at the various wavelengths to the absolutely calibrated EUV dose.[17] The supplier data here shows that the EUV resists are four times as sensitive to 157 nm radiation, meaning that 157 nm wavelengths will clear this resist four times faster than 13.5 nm radiation. In order to calculate effective flare, the bandwidth from 100-400 nm was broken up into four regions and the percent integrated power into each band was calculated from the previously determined OOB power spectral distribution profile. These values were then multiplied with the relative sensitivities to compute effective flare. The results are tabulated in table 1. For 10% OOB at IF,

Table 1: Relative resist sensitivity and effective flare

Wavelength (nm)	Relative E_o (mJ/cm^2)	Sensitivity	11 Mirrors, 10% at IF (%)	10 Mirrors, 10% at IF (%)
13.5	1.9	1x	100	100
157	0.5	4x	3.15	3.74
193	7.9	0.24x	0.35	0.42
248	2.2	1x	0.83	1.01
365	>>>13.5 nm	Very Small	Negligible	Negligible
Total effective OOB flare on pattern			**4.34**	**5.17**

the effective flare estimated by accounting for resist sensitivity in the 11 mirror and 10 mirror systems is 4.34% and 5.17% respectively. If production ready EUV lithography tools will need to achieve total flare level of less than 10% in order to meet CD control requirements, then this will be a problem and solutions will be needed.

3. 2D MASK MODEL

To examine DUV/UV flare effects on aerial image formation and to determine the validity of the estimates obtained in section 2.4, 2D aerial image modeling on a 22 nm dense mask pattern was completed. The simulation for the 0.32 optic, production type EUVL stepper assumed disk (circular) illumination with 0.5σ. We did not account for aberrations, since this data is not available. Reflection coefficients in the DUV/UV was generated using the commercial lithography simulator, PANORAMIC (ref), assuming 2.5 nm Ruthenium capping layer on multilayer stack and TaBN/TaON combined absorber thickness of 70 nm. Since the the UV plasma size will be large in comparison to the EUV plasma size, we assume incoherent illumination and this was used to model aerial images with DUV/UV wavelengths. The full 100-400 nm band was divided into four sections and the center wavelength was used as the illumination wavelength for generating aerial images.

Figure 9 shows the aerial image generated for pure EUV illumination on the left and the aerial image calculated with incoherent 137 nm illumination is shown on the right. 137 nm illuminated mask image is a third in intensity as compared to the EUV aerial image intensity. Another aspect to note is the nonuniform intensity distribution in the 137 nm image. We expect that this might have significant implications for other mask features such as contacts or isolated lines and spaces. Figure 10 shows aerial images at the four representative OOB wavelengths. As the illuminating wavelengths move into the UV, the image intensity drops and the image intensity profile is blurred significantly as we would expect.

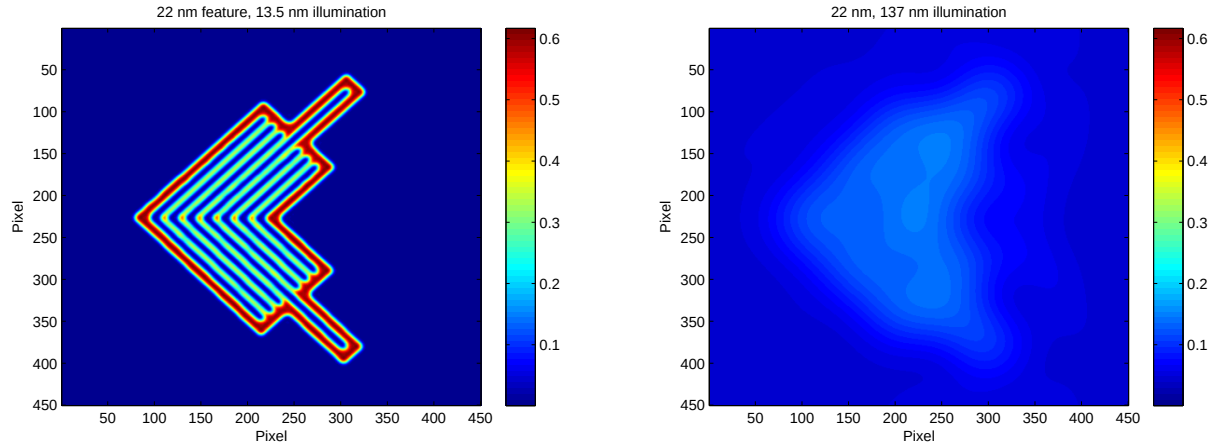

Figure 9: Compariing EUV aerial image calculated with disk illumination (left) to aerial image generated with 137 nm and incoherent illumination (right). We note large differences in image intensity.

Figure 11 show aerial images with added DUV/UV contribution according to the resist sensitivity dependence. The flare shows up as a light halo around the mask patterns. For the 10% OOB at IF, the flare calculated is 4.2% for the 11 mirrors case (fig. 11, left) and 4.98% (fig. 11, right) for the 10 mirrors case. These values are comparable to the effective flare estimated with the resist sensitivity factors in section 2.4. The flare computed from aerial images for the 20% OOB at IF for both cases approximately double from the 10% at IF case as we would expect (section 2.4). Because these wavelengths image mask pattern and since the respective image intensities vary greatly with the sensitivity of the resists to these wavelengths, we can conclude that most of the OOB flare in pattern transfer results from the bandwidth where the resists are most reactive. We also note that, treating the OOB power reaching the wafer as DC background will give a flare estimation of 6.2% (2 $\times$ the total bandwidth integrated power for the 11 mirror optical layout).

4. DUV SOURCE INTEGRATION INTO THE 0.3NA MET

The SEMATECH Berkeley 0.3 NA, EUV microfield exposure tool (MET) installed at the the Advanced Light Source synchrotron facility at Lawrence Berkeley National Laboratory currently uses a spectrally pure, debris-free, undulator radiation as the source of EUV. The MET uses programmable coherence illumination[18]and provides imaging capabilities down to 12 nm, enabling advanced resist, mask, process, and metrology methods development. Further details on the MET can be found elsewhere.[19,20] Our proposed experimental plan for enabling OOB imaging studies with MET is by incorporating a DUV/UV source of sufficient brightness and uniformity at a point in the MET optical train.

The source that was found to best match the etendue of the MET is the Laser-Driven Light Source (LDLS) EQ-1000 by Energetiq Technologies.[21] This source configuration utilizes a laser to directly heat a Xenon plasma to the temperatures necessary for deep ultraviolet production over a broad spectral range. Available wavelengths include 170 nm through visible and near IR.[21] The energy calibrated, spectral distribution from this source for available wavelengths of interest for this study is shown in figure 12 for a 1 mm aperture at source output. The measured power output at the two key resist sensitive wavelengths of 193 nm and 248 nm are 0.04 mW/nm and 0.09 mW/nm, respectively. Wavelength selection for the MET exposures is implemented with narrow bandpass filters obtained from Acton Optics & Coatings.[22] Figure 13 shows the mechanical design for incorporating the LDLS source into MET. Optical design was completed using ZEMAX, with CaF_2 aspheres utilized for collection and collimation of light from the source. The source is to be inserted above the turning mirror for the synchrotron illumination, bypassing the fly's eye mirrors and passing through the scanning illuminator. The 1 mm aperture at the source provides a source etendue small enough to support the MET NA requirements. This configuration is currently under construction and we hope to present experimental data in the near future.

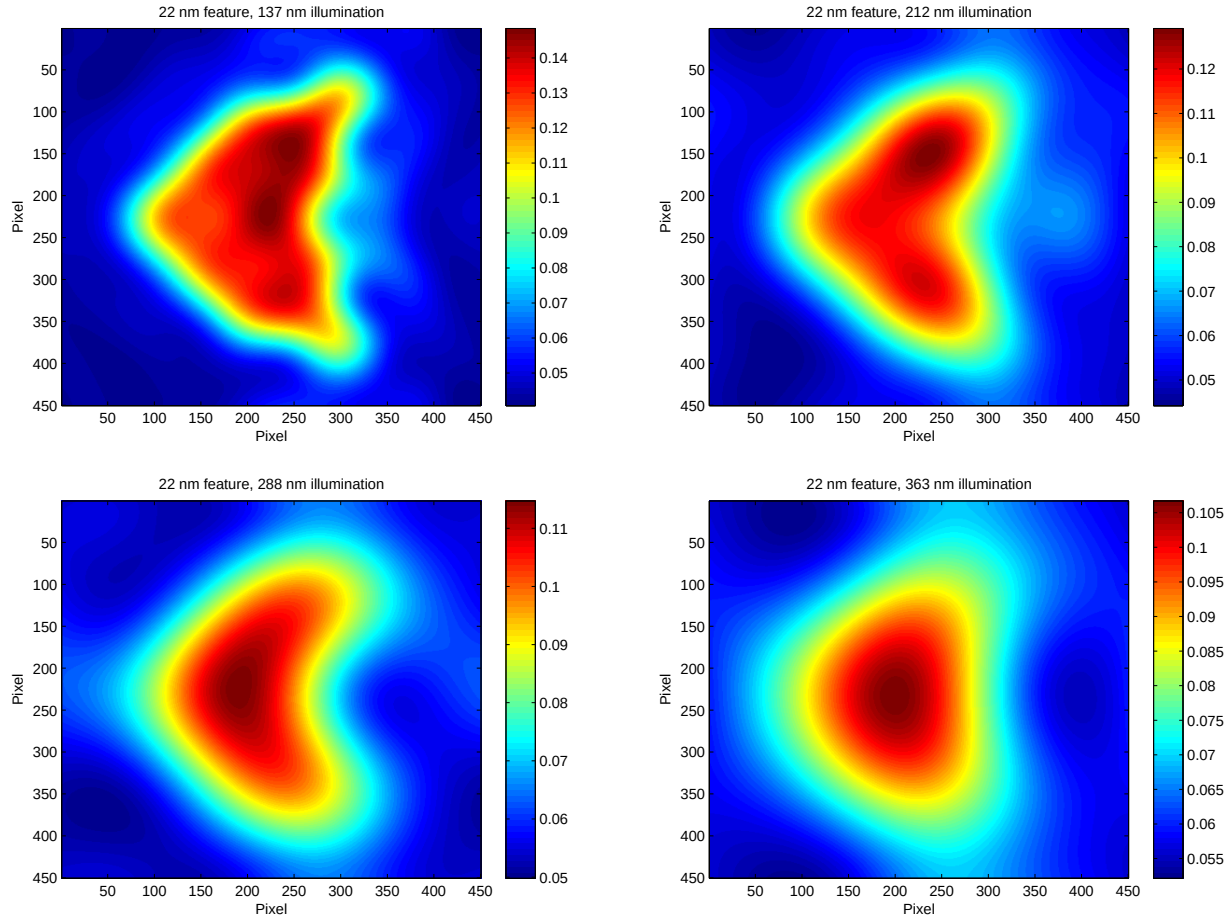

Figure 10: Aerial Images computed for the various wavelengths in the DUV/UV region. The colorbar is adjusted for contrast.

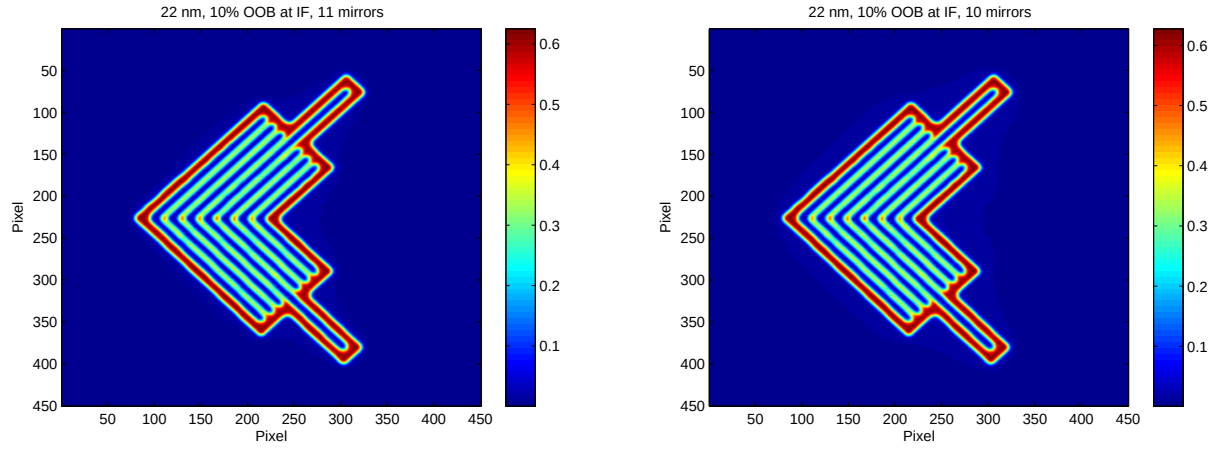

Figure 11: EUV aerial image combined with added DUV/UV contribution. For 10% OOB at IF, the flare calculated is 4.2% for the 11 mirrors case and 4.91% for the 10 mirrors case.

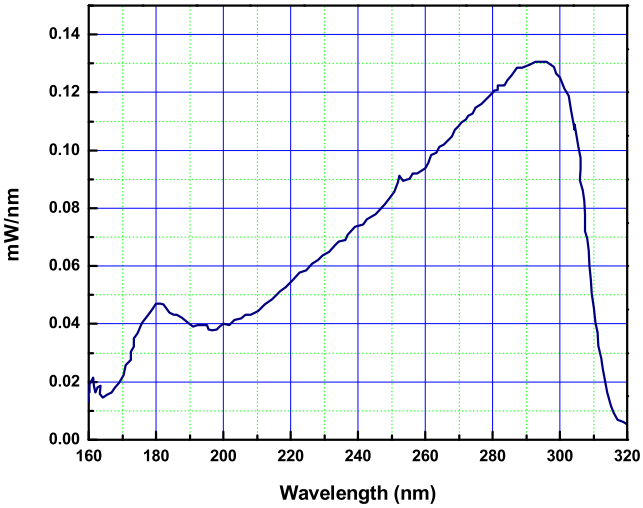

Figure 12: Energetiq LDLS EQ-1000 source power characterization at 1 mm aperture

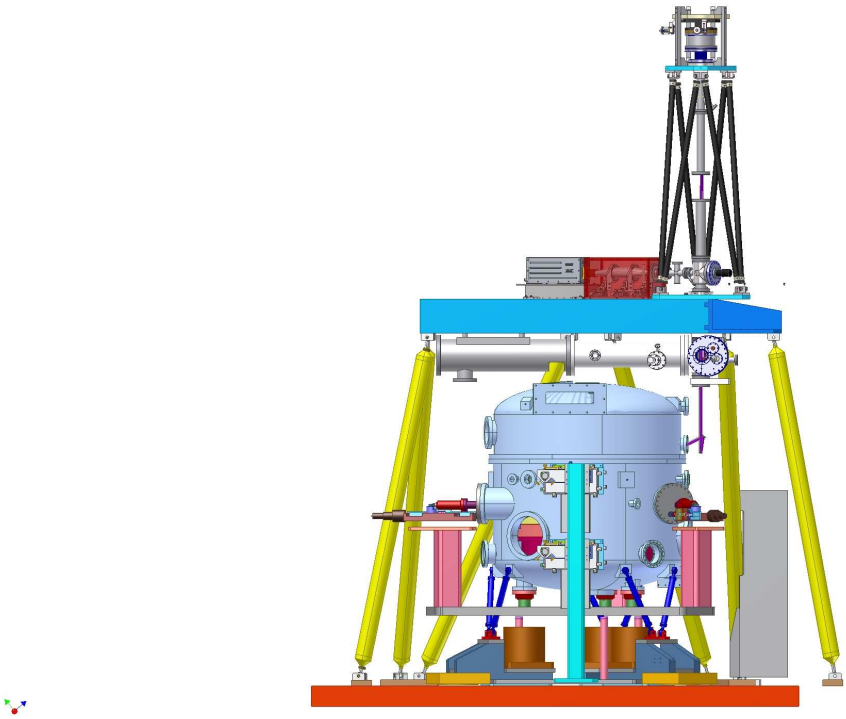

Figure 13: Proposed design for DUV/UV source input to MET

5. DISCUSSION AND SUMMARY

OOB, particularly in the DUV, is an important concern for EUVL systems. In this paper, we have presented a method for detailed estimation of flare due to the OOB DUV/UV radiation from the plasma sources collected at IF. To estimate flare effects with greater accuracy, details on the mirror characteristics, the source emission power and profile into the wavelength region of interest and the resist sensitivity characterization at wavelength, are necessary. Resist dependent flare was calculated with known resist sensitivity values relative to EUV. This effective flare contribution applied to the modeled DUV/UV aerial images, which were then added to the EUV aerial image to underscore the effect on image contrast. In a production type stepper stepper system, OOB flare in addition to the flare resulting from the low spatial frequency scatter in the optical system is expected to be significant. Solutions that have been proposed such as coatings on at least one illuminator mirror, spectral purity filters at source, etc., in order to reduce OOB radiation collected at IF will be necessary. Several flare compensation methods have also been proposed. The flare variation for features and sizes will need to be further investigated. For patterning studies with OOB radiation, we proposed integrating a DUV source into the existing SEMATECH Berkeley 0.3 NA MET. Optical and mechanical designs are now complete and construction is under way, with experimental results to be obtained shortly.

ACKNOWLEDGMENTS

The authors would like to acknowledge the support and dedication of the CXRO engineering team and staff. Useful discussions with Andrew Aquila on the MLM properties and behavior is greatly appreciated. Special thanks to the MET team members Paul Denham, Brian Hoef, and Gideon Jones. We would like to acknowledge the Energetiq team, especially Debbie Gustafson and Robert Angeli, for providing support and source spectral characterizations for this work. This work was supported by the Assistant Secretary for Energy Efficiency and Renewable Energy, Office of Building Technology, State, and Community Programs, of the U.S. Department of Energy under Contract No. DE-AC02-05CH11231.

REFERENCES

[1] Stulen, R. and Sweeney, D., "Extreme ultraviolet lithography," *Quantum Electronics, IEEE Journal of* **35**, 694–699 (May 1999).

[2] Wurm, S., Goodwin, F., and Yun, H., "Nextgeneration lithography: Euvl readiness for pilot line insertion," *Solid State Technology* **52**(2) (2009). http://www.solid-state.com/display_article/352195.

[3] Bakshi, V., ed., [*EUV Sources for Lithography*], SPIE Press, Washington (2005).

[4] Miyake, A., Kanazawa, H., Banine, V., and Suzuki, K., "Joint requirements," Presentation at EUV Workshop, Proceedings available at www.sematech.org (October 19. 2006).

[5] Kürz, P., "The euv optics development program at carl zeiss smt ag," http://www.sematech.org/meetings/archives/litho/euvl/20030930/presentations/8A%20P%20Kurz%20EUV%20Symp.pdf (2003).

[6] Naulleau, P. and Hudyma, R., "Personal communication," (February 2009). e-mail.

[7] Bruineman, C., Bijkerk, F., der Westen, S. A. V., and Bakshi, V., "Flying circus 2 (fc2): Calibration of an extreme ultraviolet (euv) source at plex llc," http://www.sematech.org/docubase/abstracts/4490atr.htm (2004).

[8] der Westen, S. A. V., Bruineman, C., Bijkerk, F., and Bakshi, V., "Flying circus 2 (fc2): Calibration of an extreme ultraviolet (euv) source at ucf," Sematech Internal Report, Unpublished (2004).

[9] Sakaguchi, H., Fujioka, S., Namba, S., Tanuma, H., Ohashi, H., Suda, S., Shimomura, M., Nakai, Y., Kimura, Y., Yasuda, Y., Nishimura, H., Norimatsu, T., Sunahara, A., Nishihara, K., Miyanaga, N., Izawa, Y., and Mima, K., "Absolute evaluation of out-of-band radiation from laser-produced tin plasmas for extreme ultraviolet lithography," *Applied Physics Letters* **92**(11), 111503 (2008).

[10] Sakaguchi, H., Fujioka, S., Namba, S., Nishimura, H., Norimatsu, T., Sunahara, A., Nishihara, K., Miyanaga, N., Izawa, Y., and Mima, K., "Spectroscopy of out-of-band radiation from laser-produced tin plasma of euv light source," (2006). http://www.ile.osaka-u.ac.jp/zone1/public/publication/apr/2006/pdf/3/3.17.pdf.

[11] Gullikson, E., "Multilayer reflectivity," (2007). http://henke.lbl.gov/optical_constants/.

[12] Palik, E. D. and Ghosh, G., [*Handbook of Optical Constants of Solids*], Academic Press, San Diego, CA (1997).

[13] Attwood, D., [*Soft X-rays and Extreme Ultraviolet Radiation: Principles and Applications*], Cambridge University Press, Berkeley (1999).

[14] cao, H., Bristol, R., Zhang, G., Yueh, W., Chandhok, M., and Kaplan, S., "Euv resist sensitivity to out of band radiation," `http://www.sematech.org/meetings/archives/litho/euvl/20041101euvl/posters/ReP10_Cao.pdf` (November 2004).

[15] Thackeray, J. W., Nassar, R. A., Brainard, R., Goldfarb, D., Wallow, T., Wei, Y., Mackey, J., Naulleau, P., Pierson, B., and Solak, H. H., "Chemically amplified resists resolving 25 nm 1:1 line: space features with euv lithography," *Emerging Lithographic Technologies XI* **6517**(1), 651719, SPIE (2007).

[16] Mbanaso, C., Denbeaux, G., Dean, K., Brainard, R., Kruger, S., and Hassanein, E., "Investigation of sensitivity of extreme ultraviolet resists to out-of-band radiation," *Emerging Lithographic Technologies XII* **6921**(1), 69213L, SPIE (2008).

[17] Naulleau, P. P., Gullikson, E. M., Aquila, A., George, S., and Niakoula, D., "Absolute sensitivity calibration of extreme ultraviolet photoresists," *Opt. Express* **16**(15), 11519–11524 (2008).

[18] Naulleau, P. P., Goldberg, K. A., Batson, P., Bokor, J., Denham, P., and Rekawa, S., "Fourier-synthesis custom-coherence illuminator for extreme ultraviolet microfield lithography," *Appl. Opt.* **42**(5), 820–826 (2003).

[19] Naulleau, P. P., Anderson, C. N., Chiu, J., Dean, K., Denham, P., Goldberg, K. A., Hoef, B., Huh, S., Jones, G., LaFontaine, B. M., Ma, A., Niakoula, D., on Park, J., and Wallow, T., "Advanced extreme ultraviolet resist testing using the sematech berkeley 0.3-na microfield exposure tool," *Emerging Lithographic Technologies XII* **6921**(1), 69213N, SPIE (2008).

[20] Naulleau, P. P., Goldberg, K. A., Anderson, E., Cain, J. P., Denham, P., Jackson, K., Morlens, A.-S., Rekawa, S., and Salmassi, F., "Extreme ultraviolet microexposures at the advanced light source using the 0.3 numerical aperture micro-exposure tool optic," *The 48th International Conference on Electron, Ion, and Photon Beam Technology and Nanofabrication* **22**(6), 2962–2965, AVS (2004).

[21] Energetiq Technology, I., "Ldls laser-driven light source eq-1000 high brightness duv light source," (2007). `http://www.energetiq.com/html/ldls.html`.

[22] Acton Optics & Coatings, a. d. o. P. I., "Optical filters," (2009). `http://www.princetoninstruments.com/products/optics/filters/default.aspx#1`.